

Computational Simulation of Composite Structural Fatigue

NASA Grant No. NAG3-2609
Clarkson University Research Project No. 375-556

Progress and Final Report

Submitted To
Dr. Christos C. Chamis
Mail Stop 49-7
National Aeronautics and Space Administration
Glenn Research Center at Lewis Field
21000 Brookpark Road
Cleveland, OH 44135

by
Levon Minnetyan
Clarkson University, Potsdam, New York 13699-5710

ABSTRACT

Progressive damage and fracture of composite structures subjected to monotonically increasing static, tension-tension cyclic, pressurization, and flexural cyclic loading are evaluated via computational simulation. Constituent material properties, stress and strain limits are scaled up to the structure level to evaluate the overall damage and fracture propagation for composites. Damage initiation, growth, accumulation, and propagation to fracture due to monotonically increasing static and cyclic loads are included in the simulations. Results show the number of cycles to failure at different temperatures and the damage progression sequence during different degradation stages. A procedure is outlined for use of computational simulation data in the assessment of damage tolerance, determination of sensitive parameters affecting fracture, and interpretation of results with insight for design decisions.

KEY WORDS: Cyclic loading, Degradation, Fatigue, Laminates, Temperature effects

INTRODUCTION

Computational simulation methods are becoming increasingly necessary for the design evaluation of composite structures. Graphite/epoxy composites are being used in many applications as airframe and engine components due to their light weight, relative low cost, and the evolution of automated fabrication processes. With the development of new constituent materials and fiber reinforcement configurations, graphite/epoxy composites are becoming more

economical for aircraft fuselage, wing, and tail substructures, engine fan blade, airbreathing components, first stage compressor, and blade containment structures. Applications of graphite/epoxy fiber composites to aircraft structures require reliable performance under fatigue loading caused by pressurization cycles, structural vibrations, and fluctuating surface pressures that develop due to the load environment. It is important to quantify the level of structural safety after damage initiation and damage growth take place in a composite structure. The relationship between damage evolution characteristics and remaining reliable life need be established for the in-service structural health monitoring.

Damage initiation and progression characteristics for composite structures are diverse. Internal damage in composites is often initiated as matrix cracking due to tensile stresses transverse to fiber orientation. At the presence of stress concentrations or defects, initial damage may also include fiber fracture. Further degradation is in the form of additional fiber fractures that usually lead to structural fracture. Because of the many possibilities with material combinations, composite geometry, fiber orientations, and loading conditions, it is essential to have an effective computational capability to predict the behavior of composite structures for any loading, geometry, composite material combinations, and boundary conditions. The predictions of damage initiation, growth, accumulation, and propagation to fracture are important in evaluating the load carrying capacity and reliability of composite structures. Quantification of the structural fracture resistance is also required to evaluate the durability/life of composite structures. A computational simulation method has been developed for this purpose. The method is able to simulate damage initiation, damage growth, and fracture in composites under various loading, considering also the effects of residual stresses and environmental conditions (Chamis et al 1996). Computational simulation has been used for the investigation of composite structures global fracture toughness (Minnetyan et al 1990), effect of the hygrothermal environment on durability (Minnetyan et al 1992), micromechanics and progressive fracture of polymer matrix composites (Gotsis et al 1997), the behavior of discontinuously stiffened composite panels under compressive loading (Minnetyan et al 1995), and damage propagation in thick composite shells under external pressure (Minnetyan and Chamis 1997). The objective of the current paper is to demonstrate a simulation capability that evaluates progressive fracture of composite structures subjected to cyclic fatigue, including the effects of temperature.

Computational simulation assumes that the complete evaluation of laminated composite fracture requires an assessment of ply and constituent material level damage/fracture processes. Computational simulation by-passes traditional fracture mechanics to provide an alternative evaluation method, conveying to the design engineer a detailed description of damage initiation, growth, accumulation, and propagation that would take place in the process of ultimate fracture of a composite structure. Results show in detail the damage progression sequence and structural response characteristics during different degradation stages. An important feature of computational simulation is the assessment of damage stability or damage tolerance of a structure under loading. At any stage of damage progression, if there is a high level of structural resistance to damage propagation under the service loading, the structure is stable with regard to fracture. The corresponding state of structural damage is referred to as *stable damage*. On the other hand, if damage progression does not encounter significant structural resistance, it corresponds to an *unstable damage* state. Unstable damage progression is characterized by very large increases in the amount of damage due to small increases in loading. On the other hand,

during stable damage progression, the amount of increase in damage is consistent with the increase in loading.

METHODOLOGY

Three distinct computer modules are combined to implement the computational simulation method. These computational modules are: (1) composite mechanics, (2) finite element analysis, and (3) damage progression tracking. The overall evaluation of composite structural durability is carried out in the damage progression module that keeps track of composite degradation for the entire structure. The damage progression module relies on a composite mechanics code (Murthy and Chamis 1986) for composite micromechanics, macromechanics, laminate analysis, as well as cyclic loading durability analysis, and calls a finite element analysis module that uses anisotropic thick shell elements to model laminated composites (Nakazawa et al 1987).

Each cycle in the simulation process begins with the definition of constituent properties from a materials databank. The composite mechanics module is called before and after each finite element analysis. Prior to each finite element analysis, the composite mechanics module computes the composite properties from the fiber and matrix constituent characteristics and the composite layup. The finite element analysis module accepts the composite properties that are computed by the composite mechanics code at each node and performs the global structural analysis at each load increment. After a finite element analysis, the computed generalized nodal force and moment time histories are supplied to the composite analysis module that evaluates the nature and amount of local damage, if any, in the plies of the composite laminate. The evaluation of local damage due to cyclic loading is based on simplified mathematical models embedded in the composite mechanics module (Murthy and Chamis 1986). The fundamental assumptions in the development of these models are the following: (1) Fatigue degrades all ply strengths at approximately the same rate (Chamis and Sinclair, 1982). (2) Fatigue degradation may be due to: (a) mechanical (tension, compression, shear, and bending); (b) thermal (elevated to cryogenic temperature); hygral (moisture); and combinations (mechanical, thermal, hygral, and reverse-tension compression). (3) Laminated composites generally exhibit linear behavior to initial damage under uniaxial and combined loading. (4) All ply stresses (mechanical, thermal, and hygral) are predictable by using linear laminate theory.

Ply failure modes are assessed by using margins of safety computed by the composite mechanics module via superposition of the six cyclic load ratios. The cyclic loads that are considered are the N_x , N_y , N_{xy} in-plane loads and M_x , M_y , M_{xy} bending moments per unit width of laminate. The lower and upper limits of the cyclic loads, the number of cycles, and the cyclic degradation parameters are supplied to the composite mechanics module at each node for the computation of a complete failure analysis based on the maximum stress criteria. Time-history dynamic analysis of structures subjected to dynamic excitation is conducted using the modal basis. Computed nodal stress resultant time-histories are used to assess the maximum and minimum values of the local load cycles and frequencies at each node. If the load cycles are applied slowly, a static analysis is conducted. The composite mechanics module with cyclic load analysis capability evaluates the local composite response at each node subjected to fluctuating stress resultants. The number of cycles required to induce local structural damage are evaluated at each node.

After damage initiation, composite properties are reevaluated based on degraded ply properties and the overall structural response parameters are recomputed. Iterative application of this computational procedure results in the tracking of progressive damage in the composite structure subjected to cyclic load increments. The number of cycles for damage initiation and the number of cycles for structural fracture are identified in each simulation. After damage initiation, when the number of load cycles reaches a critical level, damage begins to propagate rapidly in the composite structure. After the critical damage propagation stage is reached, the composite structure experiences excessive damage or fracture that causes its collapse.

Structural properties represented by the generalized stress-strain relationships are revised locally according to the composite damage evaluated after each finite element time-history analysis. The structural model is automatically updated with a new finite element mesh having reconstituted properties, and it is reanalyzed for further deformation and damage. If there is no new damage after a cyclic load increment, the structure is considered to be in equilibrium and an additional number of cycles are applied leading to possible damage growth, accumulation, or propagation. Simulation under cyclic loading is continued until structural fracture.

Structural damage may include individual ply damage and also through-the-thickness fracture of the composite laminate. The computational simulation procedure uses an accuracy criterion based on the allowable maximum number of damaged and fractured nodes within a simulation stage. If too many nodes are damaged or fractured in the simulation stage, the number of cycles is reduced and analysis is restarted from the previous equilibrium state. Otherwise, if there is an acceptable amount of incremental damage, the number of cycles is kept constant but the constitutive properties are updated to account for the damage from the previous simulation stage.

After a valid simulation step in which composite structural degradation is simulated with or without damage or fracture, the structure is reanalyzed for further damage and deformation. When there is no indication of further damage under a load, the structure is considered to have endured the previously applied cyclic loading. Subsequently, another set of cyclic loads is applied leading to possible damage growth, accumulation, or propagation. Analysis is stopped when global structural fracture is predicted.

The type of damage growth and the sequence of damage progression depend on the composite structure, loading, material properties, and hygrothermal conditions. A scalar damage variable, derived from the total volume of the structure affected by various damage mechanisms is also computed as an indicator of the level of overall damage induced by loading. This damage variable is useful for assessing the overall degradation of a given structure under a prescribed loading condition. The rate of overall damage growth during damage progression may be used to evaluate the propensity of structural fracture with increasing loading. The procedure by which the overall damage variable is computed is given by Minnetyan et al (1990).

FATIGUE DEGRADATION MODELS

The simplest degradation model is based on the assumption that all material properties may be assumed to diminish linearly on a logarithmic scale based on the number of cycles endured.

$$\frac{P}{P_0} = 1 - \beta \log N \quad (1)$$

Where P is the current value of a property, P_0 is the original value of the same property, β is the logarithmic degradation coefficient, and N is the number of load cycles. The log-linear degradation model is fairly effective in describing the cyclic fatigue response of a composite or metallic material that is loaded under a constant type of loading and uniform hygrothermal environment. A more general degradation model can be constructed to take into account temperature, state of stress, and other environmental effects. Influences of different effects on fatigue life can be represented by a Multi-Factor Interaction Model (MFIM). The fundamental premise of MFIM is that material behavior constitutes an n -dimensional space that is called Material Behavior Space (MBS) where each point represents a specific aspect of material behavior. It is further reasonable to assume that MBS can be described by an assumed interpolation function. One convenient interpolation function is a polynomial of product form because mutual interactions among different factors can be represented by the overall product, and includes those cross products in common algebraic polynomials. In this investigation, MBS is assumed to be described by the following multifactor interaction equation (MFIM):

$$\frac{M_p}{M_{P_0}} = \prod_{i=1}^N A_i^{m_i} \quad (2)$$

Where M_p is the property affected to be evaluated. M_{P_0} corresponds to the initial (reference) material state or condition. A_i represents the i th factor that influences material behavior, and m_i is an exponent. A_i is further defined by:

$$A_i = \left(1 - \frac{B}{B_0} \right)_i \quad (3)$$

Here B represents a specific cause factor for behavior (for example, temperature), and B_0 is the corresponding final value. Values for B_0 and m_i for specific behavior are selected either from known behavior or more likely from a best judgment in conjunction with consultations with seasoned professionals for that behavior.

By representing the MBS with the MFIM of product form (eq. (2)), we gain another distinct advantage. The behavior factors, B , can also be represented by another level of MFIM or progressive substructuring of equation (2). The progressive substructuring leads to a multi-tier representation of the MBS that permits intrinsic lower tier behaviors to influence more than one factor at the next higher tier. In other words, the observed specific behavior B_i may depend on another set of lower tier elemental behaviors. Further, the behavior factors in this lower set of specific behaviors may depend on yet another next lower tier of elemental behaviors. That is, there are usually sets and subsets of specific behaviors that hierarchically influence the higher level behaviors. When this is done, N can be limited to 6, (for example), but the number of factors influencing material behavior at the next lower tier will increase exponentially as N_j where j is the number of 6-factor tiers. For example, when $j = 3$, $N = 216$, and so forth. This

representation is natural for multiparallel processing computers where the tiers are programmed with different granularities. Obviously, then, the motivation for selecting such a form is for computational and programming effectiveness. Another reason for selecting an MFIM of product form is that the effect of each factor can be evaluated separately. The interpretation of B_o is that it represents a scale, whereas m_i represents a shape or path. For example, $(1 - B/B_o)^{m_i}$ where $1 > B/B_o$ and $+\infty < m_i < -\infty$ covers the whole MBS space. The inclusiveness of this particular form, combined with its simplicity, makes it very attractive for computational simulation.

COMPOSITE COUPON UNDER TENSION-TENSION FATIGUE

We consider a quasi-isotropic graphite/epoxy [45/90/-45/0], 1.0in.x6.0in. coupon that was tension-tension fatigue tested at temperatures of $t = -195, +22,$ and $+121^\circ\text{C}$ by Uleck et al (1998). Figure 1 compares the log-linear degradation described by the logarithmic decrement model for the quasiisotropic graphite/epoxy composite subjected to 22°C room temperature cyclic loading at different load amplitudes with corresponding test data. The logarithmic degradation coefficient β is 0.06 in Figure 1. The model is a good log-linear fit to the test data. However, the logarithmic decrement model is not able to distinguish between the different temperatures. To take the temperature effects into account, the Multi-Factor Interaction Model is set up in the form of:

$$\frac{P}{P_o} = \left(\frac{t_{gw} - t}{t_{gw} - t_o}\right)^{m_t} \left(1 - \frac{\sigma}{S}\right)^{m_s} \left(1 - \left\{\frac{t_{gw} - t}{t_{gw} - t_o}\right\}^{m_{tn}} \frac{\sigma_M N_M}{S.N_{Mf}}\right)^{m_n}$$

Where $t_{gw}=204^\circ\text{C}$, $t_o=21^\circ\text{C}$, $S=98 \text{ Mpa}$, $N_{Mf}=100000$, $m_t=0.5$, $m_s=0.5$, $m_n=0.75$, $m_{tn}=0.75$ for $t > 22^\circ\text{C}$, $m_{tn}=0$ for $t < 22^\circ\text{C}$. Figure 2 compares the MFIM simulation results with the test data for all three temperatures. The MFIM based computational simulation was able to include the temperature effects in a single MFIM equation inserted into the composite mechanics durability analysis module. The agreement between computational simulations and test data is reasonable for preliminary design investigations under fatigue loading. The AS-4 graphite fiber properties used in the simulation are given in Table 1 and the intermediate modulus Epoxy matrix properties are given in Table 2.

COMPOSITE CYLINDRICAL SHELL UNDER PRESSURIZATION CYCLES

An example application of the MFIM simulation is the pressurization cycles of a quasiisotropic [45/90/-45/0]s graphite/epoxy composite cylindrical shell. The cylindrical shell has a length of $L=760 \text{ mm}$, a diameter of $d=305 \text{ mm}$, and a thickness of $t=1.27 \text{ mm}$. The finite element model has 544 nodes and 512 shell elements as shown in Figure 3. Pressurization of the closed end shell is simulated by adding axial tension such that the axial stresses are half those of the hoop stresses. Figure 4 shows the MFIM simulations for the three temperatures considered. For all three temperatures the damage progression characteristics may be outlined by the following stages:

1. Damage initiation is by transverse tensile failures in the 0° plies.
2. Damage growth is by longitudinal compressive failures of the 0° plies due to the weakened matrix support.
3. Damage accumulation is by transverse tensile failures of the 90° and ±45° plies.
4. Damage propagation by the longitudinal compressive failure of the 90° plies.
5. Structural fracture occurs by the longitudinal tensile failures of the surface +45° plies.

The reduction of the number of cycles to failure at high temperatures is mainly due to the inability of the material to dissipate the generated hysteretic internal energy and the additional deformability of the material at the higher temperature. At the low temperature of -195°C, even though the material becomes brittle, its cyclic energy is reduced and the ability to dissipate the energy is improved, thereby extending the fatigue life. The simulation of composite shell pressurization fatigue is conservative due to the beneficial effects of the biaxial tension stress state.

COMPOSITE AIRFOIL UNDER LOADING

A graphite/epoxy laminated cantilever airfoil is used to demonstrate the fatigue simulation of a composite structure subjected to flexural loading. The airfoil has a length of 1829 mm (72.0 in) and the width varies from 102 mm (4.0 in) at the tip to 76 mm (3.0 in) at the base. The ply layup is $[0_3/18/-18/90/-18/18/0_3]_n$. The laminate thickness is 79 mm (3.10 in) at the root and 7.0 mm (0.275 in) at the blade tip. The finite element model of the airfoil contains 160 elements and 187 nodes as shown in Figure 5.

The composite system is made of AS-4 graphite fibers in a high-modulus, high strength (5250) epoxy matrix. The fiber and matrix properties corresponding to this case are given in Tables 1 and 3, respectively. Matrix properties are representative of the Rigidite-5250 high temperature resin. The fiber volume ratio is 0.55 and the void volume is assumed to be zero.

The airfoil is first investigated subjected to a monotonically increasing lateral pressure applied at room temperature of 22°C. Damage propagation is simulated as the lateral pressure is increased. Figure 6 shows the percent damage volume in the airfoil with increasing lateral pressure. Damage initiation occurs at a lateral pressure of approximately 13.8 kPa (2.0 psi). The damage initiation mode is by transverse tensile failure of the 90° plies near the root. After damage initiation, the damage growth rate with pressure remains steady until the critical pressure level of 41.4 kPa (6.0 psi) is reached. Above the 41.4 kPa pressure level damage propagates very suddenly with fiber fractures that cause the airfoil to break into two pieces. Figure 7 shows the airfoil tip deflection with increasing lateral pressure. The relationship between pressure and tip deflection is linear until the critical damage propagation pressure of 41.4 kPa is reached. Figure 8 shows the exhausted damage energy as a function of the created damage volume. The relationship between damage volume and damage energy is linear until the critical damage level is reached. After the critical damage level, the exhausted damage energy grows much more rapidly compared to the damage volume. This critical damage stage is also called the damage tolerance limit of the composite structure. Figure 9 shows the Damage Energy Release Rate

(DERR) that is defined as the rate of work done by external pressure during the evolution of damage to the damage volume created. Fluctuations in the DERR levels correspond to the changes in the structural resistance to damage propagation.

After simulation of the airfoil under monotonically increasing static loading, its durability under fatigue loading was investigated. The pressure amplitude for fatigue was selected approximately halfway between the damage initiation and damage propagation pressures. The fatigue pressure of 27.6 kPa (4.0 psi) was applied with zero stress ratio, without stress reversal. The damage evolution characteristics were tracked with increasing number of pressure cycles. Figure 10 shows the created damage with number of fatigue cycles. The damage volume increases rapidly within the first few cycles. Afterwards, the increase in the damage volume becomes more and more gradual with the increasing number of cycles. However, at the end of the fatigue life, the small changes in the damage volume represent larger steps in approaching the damage tolerance limit. Figure 11 shows the relationship between the fatigue damage energy exhausted and the created damage volume. At the end of the fatigue life the slope of the damage energy curve becomes practically infinite. Accordingly, the damage volume alone is not a sufficient indicator to identify the damage tolerance limit under fatigue. Similarly the changes in airfoil tip deflection with the number of fatigue cycles, as shown in Figure 12, do not provide any warning of the impending ultimate failure. Figure 13 shows the DERR with increasing number of fatigue cycles. There is a rapid increase in the DERR levels immediately before ultimate fracture. Therefore, any diagnostic methodology for structural health monitoring must be able to measure both the increase in damage volume and also the exhausted damage energy. Adequate warning before failure may be obtained by comparison of measured damage and damage energy levels to the corresponding simulated values.

GENERALIZATION OF PROCEDURE

The present computational simulation method is suitable for the design and continued in-service evaluation of composite structures subjected to cyclic loading. Composite structures with different constituents and ply layups can be evaluated under cyclic loading and pressurization. The cyclic load amplitude and the environmental temperature may be varied during the simulated fatigue life. Static and dynamic load combinations may also be applied in addition to cyclic loading.

Structural health monitoring is based on damage tolerance requirements defined via the computational simulation method. A cyclic fatigue damage tolerance parameter is described as the state of damage and the exhausted damage energy after the application of a given number of loading cycles, normalized with respect to the damage state corresponding to ultimate fracture. Identification of damage progression mechanisms and the sequence of progressive fracture modes conveys useful information to evaluate structural safety. Computational simulation results can be formulated into health monitoring criteria, increasing the reliability of composite structures. The simulated failure modes and the type of failure provide the necessary quantitative and qualitative information to design an effective health monitoring system. Computed local damage energy release rates are correlated with the magnitudes of acoustic emission signals and other damage monitoring means such as piezoelectric stress sensors and

strain gages that are an integral part of the monitored composite structure. Fiber optics data networks embedded in the composite structure would transmit the detected local damage information to an expert system that provides feedback and reduces engine power to delay failure.

The basic procedure is to simulate a computational model of the composite structure subjected to the expected loading environments. Various fabrication defects and accidental damage may be represented at the ply and constituent levels, as well as at the laminate level. Computational simulation may be used to address various design and health monitoring questions as follows:

1. **Evaluation of damage tolerance:** Computational simulation will generate the damage that would be caused due to cyclic fatigue damage or overloading by the type of load the structure is designed to carry. On the other hand, a fabrication defect or accidental damage produced by inadvertent loading that is not an expected service load can be included in the initial computational model. Once the composite damage is defined, damage tolerance can be evaluated by monitoring damage growth and progression from the damaged state to ultimate fracture. Significant parameters that quantify damage stability and fracture progression characteristics are the rate of damage increase with incremental loading, and the changes in the exhausted damage energy with loading. Identification of damage initiation/progression mechanisms and the sequence of progressive fracture modes convey serviceable information to help with critical decisions in the structural design and health monitoring process. Determination of design allowables based on damage tolerance requirements is an inherent use of the computational simulation results. Simulation of progressive fracture from defects allows setting of quality acceptance criteria for composite structures as appropriate for each functional requirement. Detailed information on specific damage tolerance characteristics help establish criteria for the retirement of a composite structure from service for due cause.
2. **Determination of sensitive parameters affecting structural fracture:** Computational simulation indicates the damage initiation, growth, and progression modes in terms of a damage index that is printed out for the degraded plies at each damaged node. In turn, the damage index points out the fundamental physical parameters that characterize the composite degradation. For instance, if the damage index shows ply transverse tensile failure, the fundamental physical parameters are matrix tensile strength, fiber volume ratio, matrix modulus, and fiber transverse modulus, of which the most significant parameter is the matrix tensile strength (Murthy and Chamis, 1986). In addition to the significant parameters pointed out by the ply damage index, sensitivity to hygrothermal parameters may be obtained by simulating the composite structure at different temperatures and moisture contents. Similarly, sensitivity to residual stresses may be assessed by simulating the composite structure fabricated at different cure temperatures. Identification of the important parameters that significantly affect structural performance for each design case allows optimization of the composite for best structural performance. Sensitive parameters may be constituent strength, stiffness, laminate configuration, fabrication process, and environmental factors.

3. Interpretation of experimental results for design decisions: Computational simulation allows interactive experimental-numerical assessment of composite structural performance. Simulation can be used prior to testing to identify locations and modes of composite damage and released damage energy that need be monitored by proper instrumentation and inspection of the composite structure. Interpretation of experimental data can be significantly facilitated by detailed information from computational simulation. Subscale experimental results may be extended to full prototype structures without concern for scale effects since computational simulation does not presume any global parameters but is based on constituent level damage tracking.

CONCLUSIONS

On the basis of the results obtained from the investigated composite airfoil example and from the general perspective of the available computational simulation method, the following conclusions are drawn:

1. The number of cycles to structural failure can be evaluated via computational simulation.
2. Effects of different temperatures can be taken into account using a multi-factor interaction model.
3. Computational simulation can be used to track the details of damage initiation, growth, and subsequent propagation to fracture for composite structures subjected to cyclic fatigue.
4. For the example angleplied composite airfoil structure considered, critical changes in the damage evolution characteristics can be identified by monitoring the damage growth and the associated damage energy.
5. Computational simulation, with the use of established composite mechanics and finite element modules, can be used to predict the influence of composite geometry as well as loading and material properties on the durability of composite structures.
6. The demonstrated procedure is flexible and applicable to all types of constituent materials, structural geometry, and loading. Hybrid composites and homogeneous materials, as well as laminated, stitched, woven, and braided composites can be simulated.
7. A new general methodology has been demonstrated to investigate damage propagation and progressive fracture of composite structures due to cyclic loading.

REFERENCES

1. C.C. Chamis, P.L.N. Murthy, and L. Minnetyan (1996) "Progressive Fracture of Polymer Matrix Composite Structures," Theoretical and Applied Fracture Mechanics, Vol. 25, pp. 1-15

2. L. Minnetyan, P.L.N. Murthy, and C.C. Chamis (1990) "Composite Structure Global Fracture Toughness via Computational Simulation," Computers & Structures, Vol. 37, No. 2, pp.175-180
3. L. Minnetyan, P.L.N. Murthy, and C.C. Chamis (1992)"Progressive Fracture in Composites Subjected to Hygrothermal Environment," International Journal of Damage Mechanics, Vol. 1, No. 1, pp. 60-79
4. P.K. Gotsis, C.C. Chamis, and L. Minnetyan (1997)"Prediction of Composite Laminate Fracture: Micromechanics and Progressive Fracture," Composites Science and Technology, Vol. 57
5. L. Minnetyan, J.M. Rivers, C.C. Chamis, and P.L.N. Murthy (1995) "Discontinuously Stiffened Composite Panel under Compressive Loading," Journal of Reinforced Plastics and Composites, Vol. 14, No. 1, pp. 85-98.
6. L. Minnetyan and C.C. Chamis (1997) "Progressive Fracture of Composite Cylindrical Shells Subjected to External Pressure," ASTM Journal of Composite Technology and Research, Vol. 19, No. 2, pp. 65-71
7. P.L.N. Murthy and C.C. Chamis (1986) Integrated Composite Analyzer (ICAN): Users and Programmers Manual, NASA Technical Paper 2515
8. S. Nakazawa, J.B. Dias, and M.S. Spiegel (1987) MHOST Users' Manual, Prepared for NASA Lewis Research Center by MARC Analysis Research Corp.
9. C. C. Chamis and J. H. Sinclair (1982)"Durability/Life of Fiber Composites in Hygrothermomechanical Environments," Composite Materials, Testing and Design, I. M. Daniel, Ed., ASTM STP-787, ASTM, Philadelphia, pp. 498-512
10. K. R. Uleck, J. S. Harris, and A. J. Vizzini, (1998) "Effect of Temperature on the Fatigue Life of a Quasi-Isotropic Gr/Ep Laminate," Proceedings of the American Society of Composites 13th Annual Technical Conference on Composite Materials, September 21-23, Baltimore, Maryland, 8p.

BIOGRAPHY

Dr. Levon Minnetyan is a professor of structural engineering at Clarkson University in the Department of Civil and Environmental Engineering. His primary research activities are directed toward the assessment of progressive damage and fracture in structures made of composite materials such as graphite/epoxy laminated, woven, and braided composites.

TABLE 1: AS-4 Fiber Properties:

Number of fibers per end = 10000
Fiber diameter = 0.00762 mm (0.300E-3 in)
Fiber Density = 4.04E-7 Kg/m³ (0.063 lb/in³)
Longitudinal normal modulus = 227 GPa (32.90E+6 psi)
Transverse normal modulus = 13.7 GPa (1.99E+6 psi)
Poisson's ratio (ν_{12}) = 0.20
Poisson's ratio (ν_{23}) = 0.25
Shear modulus (G_{12}) = 13.8 GPa (2.00E+6 psi)
Shear modulus (G_{23}) = 6.90 GPa (1.00E+6 psi)
Longitudinal thermal expansion coefficient = -1.0E-6/°C (-0.55E-6 /°F)
Transverse thermal expansion coefficient = 1.0E-5/°C (0.56E-5 /°F)
Longitudinal heat conductivity = 43.4 J-m/hr/m²/°C (580 BTU-in/hr/in²/°F)
Transverse heat conductivity = 4.34 J-m/hr/m²/°C (58 BTU-in/hr/in²/°F)
Heat capacity = 0.712 KJ/Kg/°C (0.17 BTU/lb/°F)
Tensile strength = 3.723 GPa (540 ksi)
Compressive strength = 3.351 GPa (486 ksi)

TABLE 2: Intermediate Modulus Epoxy Matrix Properties:

Matrix density = 3.27E-7 Kg/m³ (0.0440 lb/in³)
Normal modulus = 3.65 GPa (530 ksi)
Poisson's ratio = 0.35
Coefficient of thermal expansion = 0.648E-4/°C (0.360E-4 /°F)
Heat conductivity = 0.654E-3 J-m/hr/m²/°C (0.868E-8 BTU-in/hr/in²/°F)
Heat capacity = 1.047 KJ/Kg/°C (0.25 BTU/lb/°F)
Tensile strength = 110.9 MPa (15.5 ksi)
Compressive strength = 242 MPa (35.0 ksi)
Shear strength = 89.7 MPa (13.0 ksi)
Allowable tensile strain = 0.02
Allowable compressive strain = 0.05
Allowable shear strain = 0.035
Allowable torsional strain = 0.035
Void conductivity = 16.8 J-m/hr/m²/°C (0.225 BTU-in/hr/in²/°F)
Glass transition temperature = 216°C (420°F)

TABLE 3: 5250 HMHS Matrix Properties:

Matrix density = 3.40E-7 Kg/m³ (0.0457 lb/in³)
Normal modulus = 4.62 GPa (671 ksi)
Poisson's ratio = 0.705
Coefficient of thermal expansion = 0.518E-4/°C (0.288E-4 /°F)
Heat conductivity = 0.649E-3 J-m/hr/m²/°C (0.862E-8 BTU-in/hr/in²/°F)
Heat capacity = 1.047 KJ/Kg/°C (0.25 BTU/lb/°F)

Tensile strength = 75.1 MPa (10.9 ksi)
 Compressive strength = 283 MPa (41.0 ksi)
 Shear strength = 138 MPa (20.0 ksi)
 Allowable tensile strain = 0.02
 Allowable compressive strain = 0.05
 Allowable shear strain = 0.04
 Allowable torsional strain = 0.04
 Void conductivity = 16.8 J-m/hr/m²/°C (0.225 BTU-in/hr/in²/°F)
 Glass transition temperature = 216°C (420°F)

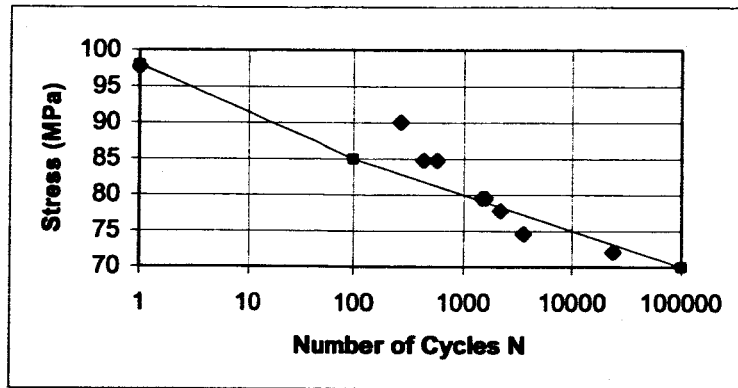


Figure 1 Logarithmic Decrement Model for Cyclic Fatigue ($\beta=0.06$)

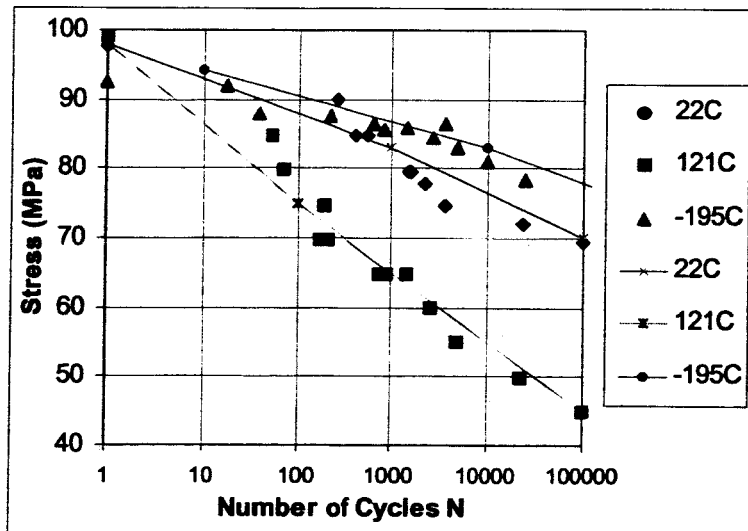


Figure 2 MFIM for Cyclic Fatigue at Different Temperatures

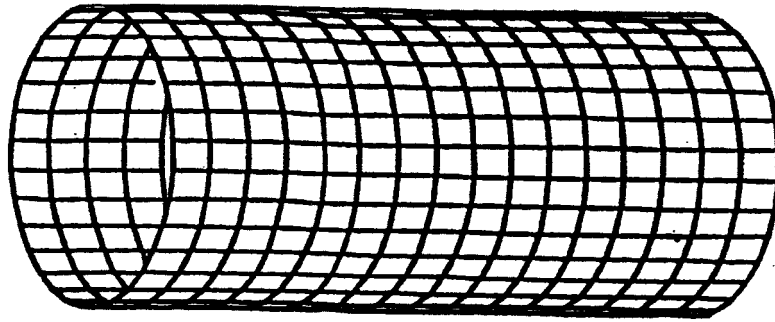


Figure 3 Finite Element Model of Cylindrical Shell

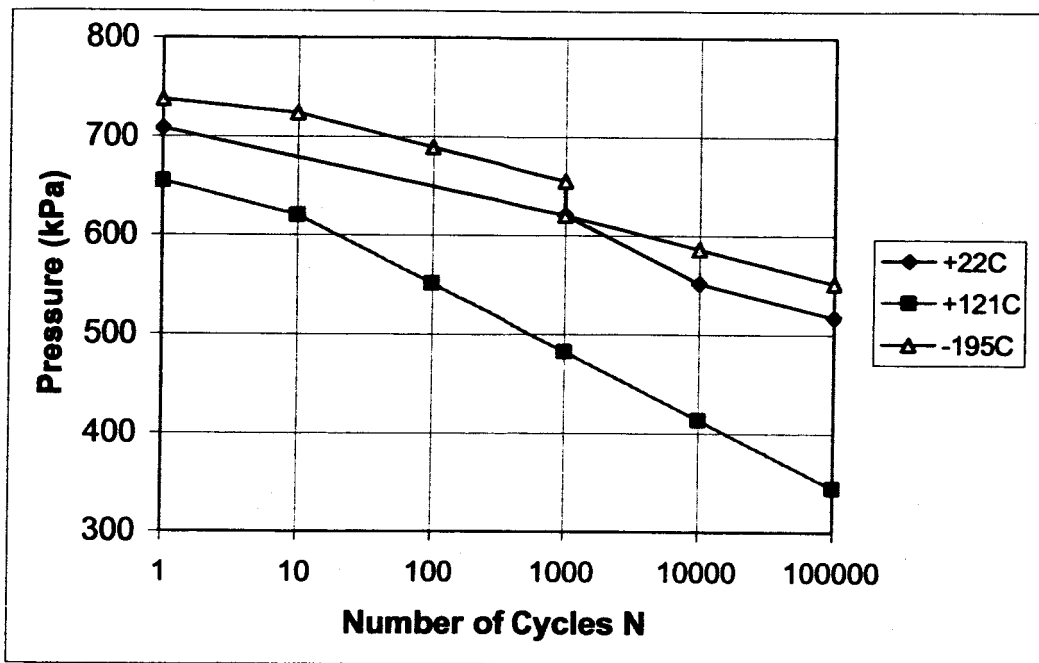


Figure 4 MFIM Simulations of Composite Shell Fatigue

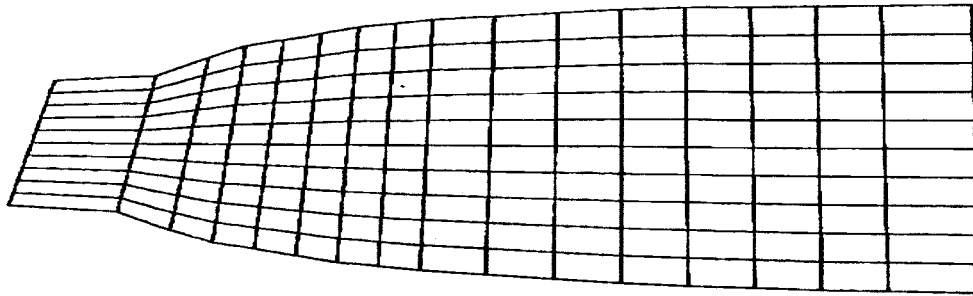


Figure 5-Finite element model of airfoil structure

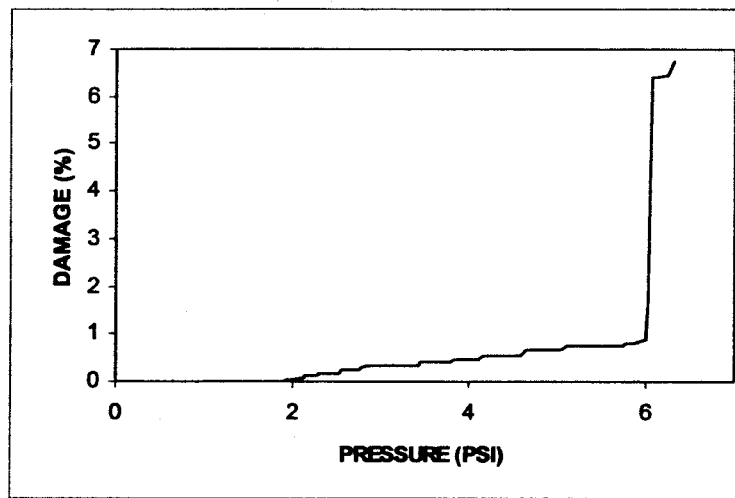


Figure 6-Damage progression in composite airfoil under static pressure

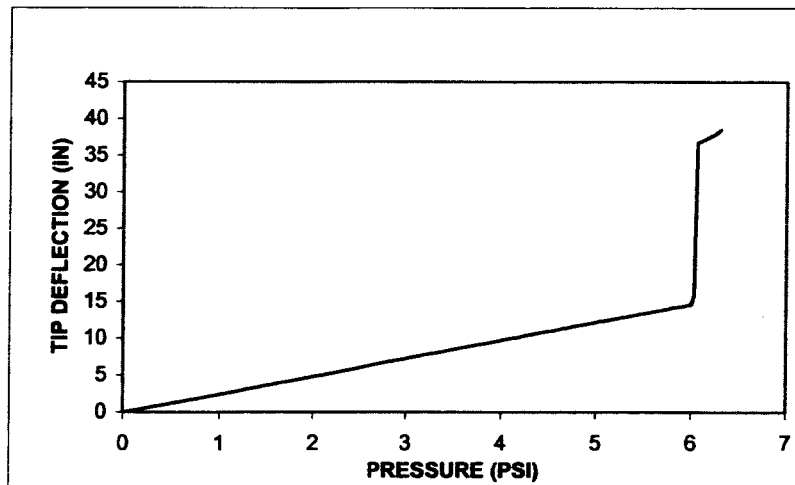


Figure 7-Deflection of airfoil tip with pressure

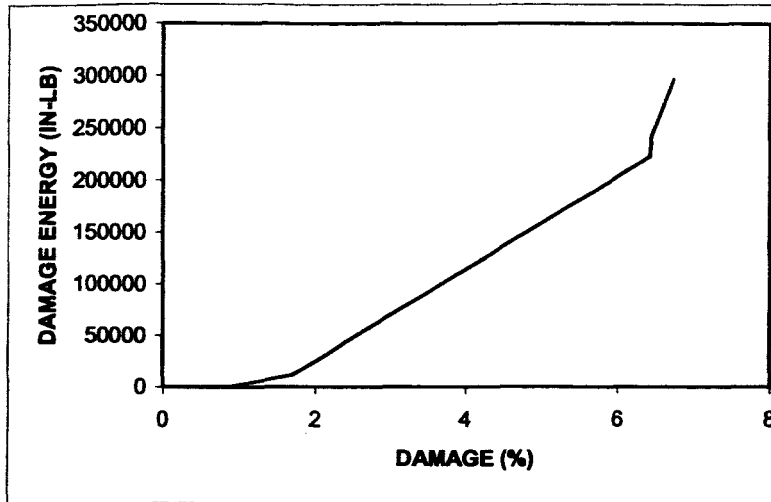


Figure 8-Airfoil damage energy exhausted with damage volume created

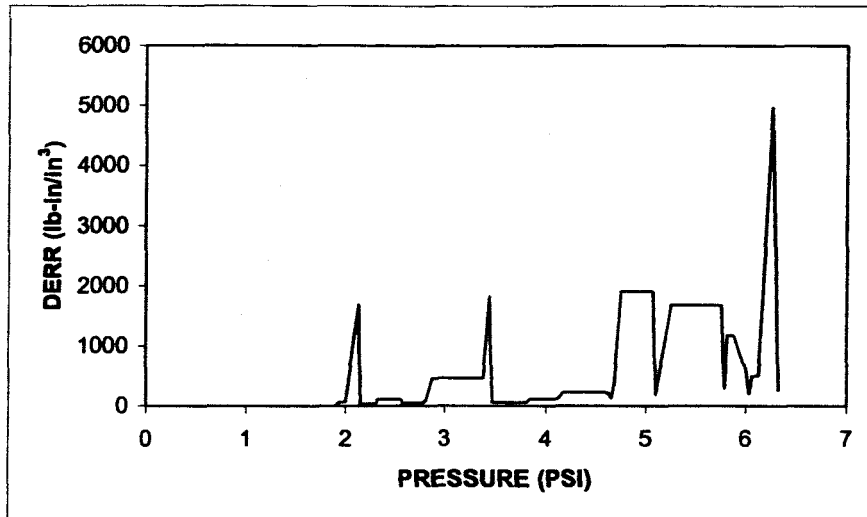


Figure 9-Airfoil damage energy release rates with pressure

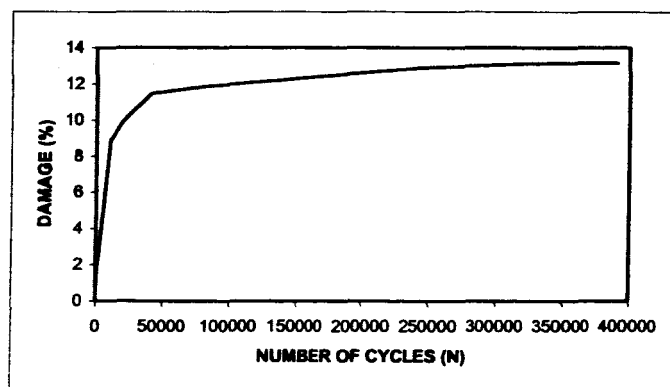


Figure 10-Airfoil damage evolution with number of fatigue cycles

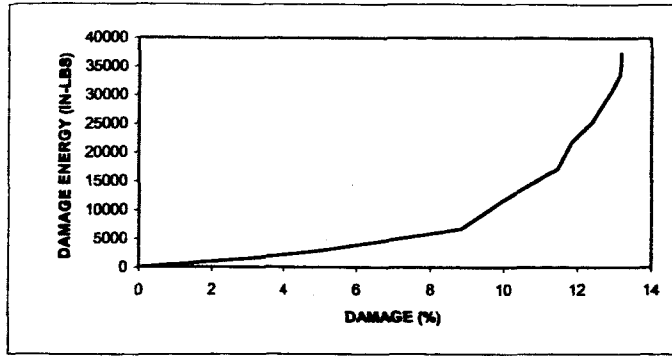


Figure 11-Fatigue damage energy exhausted with percent damage volume

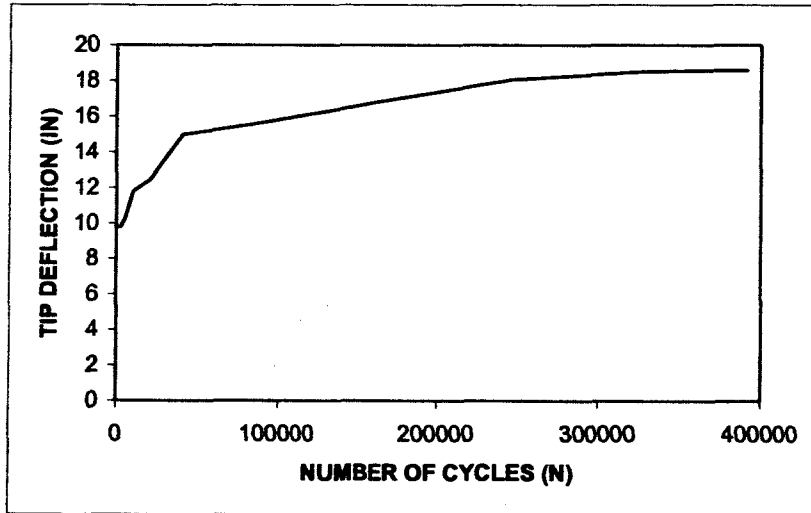


Figure 12-Airfoil tip deflection with number of pressurization cycles

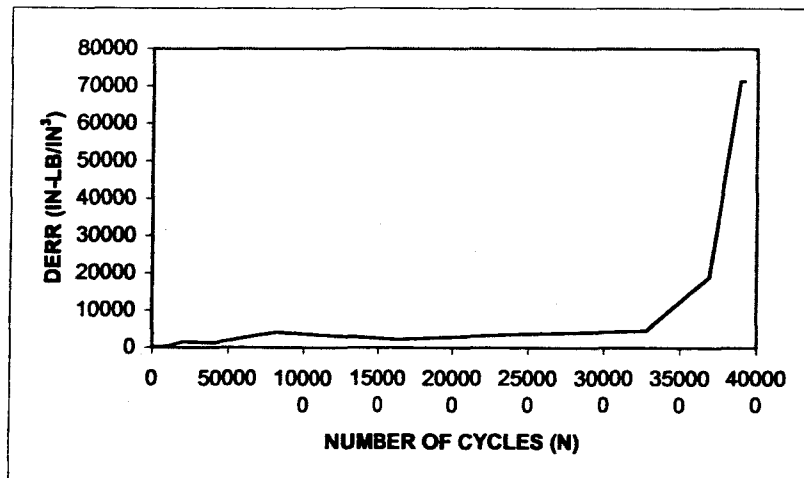


Figure 13-Airfoil damage energy release rate with number of fatigue cycles